10/3-5-90 J SD

SANDIA REPORT

SAND90-8200
Unlimited Release
Printed January 1990

Radiation-Induced Density Changes and Creep in Surface Layers of Glass

W. G. Wolfer, A. J. Antolak

Prepared by
Sandia National Laboratories
Albuquerque, New Mexico 87185 and Livermore, California 94550
for the United States Department of Energy
under Contract DE-AC04-76DP00789

Issued by Sandia National Laboratories, operated for the United States Department of Energy by Sandia Corporation.

SAND--90-8200

SAND90-8200
Unlimited Release
Printed January 1990

DE90 008112

Radiation-Induced Density Changes and Creep in Surface Layers of Glass

W. G. Wolfer and A. J. Antolak
Theoretical Division
Sandia National Laboratories
Livermore, CA 94551

ABSTRACT

When glass surfaces are bombarded by energetic charged particles, radiation-induced density changes happen within the damaged surface layer. As a result of the lateral constraints imposed by the undamaged substrate material, stresses are also generated within the damaged layer. A detailed analysis of the stress evolution is given together with an analysis of the surface displacement and the bending of plate-like specimens bombarded from one side. The damaged material is assumed to deform as a viscoelastic material with a power-law stress dependence. The results of this analysis are applied to earlier experimental results in order to extract creep parameters which describe this viscoelastic and radiation-induced deformation in hydrogen-free vitreous silica.

I. INTRODUCTION

Radiation damage in solids frequently produces density changes with increasing dose. In crystalline metals, the phenomenon of radiation-induced swelling has been extensively studied over the last two decades, and it has been found that it is caused by the agglomeration of point defects, namely self-interstitials and vacancies, which are created by displacement damage. The agglomeration involves the diffusion of these point defects to larger defects such as dislocation loops and voids. In the case of metals, the density decreases with increasing dose. However, in graphite the initial density change is compaction, followed later by a density decrease. This more complicated behavior can be explained with the anisotropic radiation-induced shape change of the graphite crystallites which make up a graphite composite. Nevertheless, the fundamental primary defects produced by the radiation are again self-interstitials and vacancies which agglomerate by diffusion to form larger defects. Radiation damage in ceramic and ionic solids is even more difficult to understand in terms of elementary defects because of the charge state of the latter. However, density changes are again a general observation rather than an exception. The common denominator of all radiation-induced density changes is simply the rearrangement of atoms and chemical bonds which make up the solid.

This rearrangement of atoms and bonds can also be influenced by external and internal stresses such that shape changes occur in addition to density changes. These stress-biased and radiation-induced shape changes can in fact be viewed as radiation-induced creep, and this phenomenon has also been extensively studied over the last decade in both metallic and ceramic crystalline solids. In metals, theoretical predictions [1] compare favorably with experimental results, indicating that a good understanding has been reached of this phenomenon in crystalline solids. For these materials, radiation-induced creep is as pervasive a phenomenon as is radiation-induced swelling and compaction, and the two have, in fact, a common origin. Nevertheless, radiation-induced creep can happen even without swelling or compaction, and must therefore be considered as an additional radiation-induced phenomenon.

Based on these general observations, it is then reasonable to assume that radiation-induced creep is also occurring in glasses, and that it accompanies the radiation-induced density changes. Even though there exists no direct experimental evidence for this proposition, some circumstantial evidence has been provided by the

work of Primak [2] and Dellin, Tichenor, and Barsis [3]. Primak [2] measured the step height between a surface region bombarded with low energy protons or helium ions and an adjacent region not subject to irradiation. He found that for quartz, the step height corresponded to swelling of the irradiated surface region, whereas a depression or compaction was found for vitreous silica. The step height correlated with the total density change even though it occurred apparently only in the direction perpendicular to the surface. He concluded therefore that radiation-induced plastic flow must direct the density change into the unrestrained direction. Dellin, Tichenor, and Barsis [3] measured both the density change and the stresses associated with them in the surface layer of vitreous silica bombarded by 18-kev electrons. They found that the stresses generated at low doses are entirely because of the isotropic density changes in the radiation-damaged layer, but at higher doses they become less than inferred from the larger density changes. They interpreted these findings in terms of two components for the density change; an isotropic part giving rise to stresses, and an anisotropic one generating no stresses. The first component saturates at a low dose, where the second component begins to evolve and becomes predominant at higher doses. It will be shown in the present paper that radiation-induced creep provides an alternate, and perhaps more natural, explanation for these findings. In the next section, we develop the mathematical formalism for the stresses produced in the irradiated layer. Section III implements the measurements of Dellin et al. [3] on hydrogen-free vitreous silica into this formalism; the last section summarizes our results.

II. STRESSES GENERATED IN THE BOMBARDED LAYER

The specimens used in the above mentioned experiments have the geometry of thin plates of thickness, h, as illustrated in Fig.1. The range, δ, of the energetic charged particles employed is approximately a few μm, and therefore much smaller than the plate thickness and the lateral extension or width of the bombarded surface layer. Since any plane cross section perpendicular to the plate surface can be assumed to remain plane and perpendicular, the total strains, ε_{11} and ε_{22}, in the directions parallel to the specimen surface are given by

$$\varepsilon_{11} = \varepsilon_{22} = K + Lz \qquad (1)$$

where K is the average lateral strain and L the curvature of the plate. The state of stress formed in the plate as a result of density changes in the surface layer is one of plane, biaxial stress, i.e.,

$$\sigma_{33} = \sigma_{32} = \sigma_{31} = \sigma_{12} = 0 \qquad (2)$$

$$\sigma_{11} = \sigma_{22} = \sigma(z) \qquad (3)$$

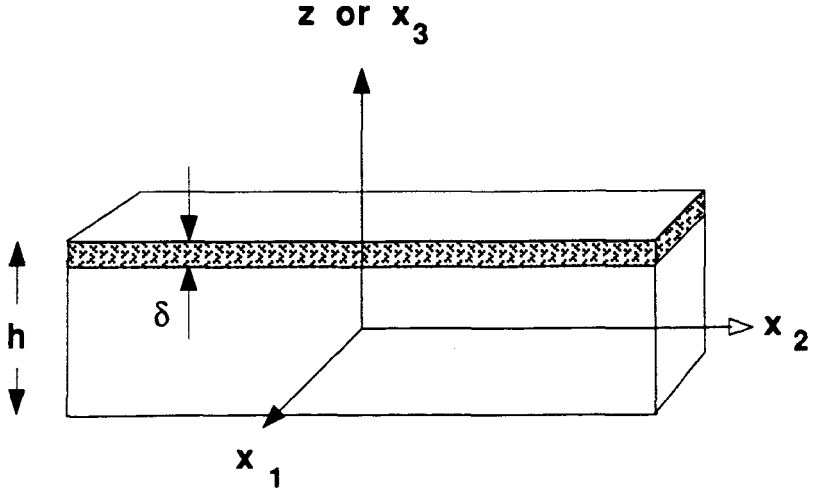

Fig. 1. Specimen geometry with coordinates and bombarded surface layer.

The rate of change of the compaction and the creep strains in the bombarded layer are related by the constituitive law

$$\frac{de_{ij}}{dR} = \frac{1}{3}\delta_{ij}\frac{dS}{dR} + \Psi(R, \sigma_{eq})s_{ij} \qquad (4)$$

where

$$s_{ij} = \sigma_{ij} - \frac{1}{3}\delta_{ij}\sigma_{kk} \qquad (5)$$

is the deviatoric stress tensor. In eqn. (4), e_{ij} are components of the inelastic strain tensor, dS/dR is the derivative of fractional volume change with respect to the dose R, δ_{ij} is the Kronecker delta tensor, and Ψ is the creep compliance or the inverse of the viscosity. In general, we expect Ψ to depend on the material, its density, and if the viscous flow of glass under irradiation is non-Newtonian, it will also depend on the equivalent stress σ_{eq}.

The first term in eqn. (4) is due to the density change assumed to be isotropic, and it represents the strains associated with compaction (negative S) or swelling (positive S). The second term represents the radiation-induced creep strain rate, and its dependence on the deviatoric stress tensor s_{ij} ensures that no density changes are caused by creep deformation.

The elastic strains in the bombarded layer are equal to the difference in the total strains ε_{ij} and the inelastic strains eij, and they are related to the stresses by Hooke's law

$$\varepsilon_{ij} - e_{ij} = \frac{1}{E}\left[(1+\nu)\sigma_{ij} - \nu\delta_{ij}\sigma_{kk}\right] \qquad (6)$$

where E is the Young's modulus and ν the Poisson's ratio. In addition, the lateral stress component $\sigma(z)$ must satisfy the equilibrium conditions

$$N = \int_{-h/2}^{h/2} \sigma(z)dz \qquad (7)$$

and

$$M = \int_{-h/2}^{h/2} \sigma(z)zdz \qquad (8)$$

where N and M is the applied membrane load and bending moment, respectively. Using the above results, it can be shown [4] that

$$K = \frac{1-\nu}{Eh} N + \frac{1}{h} \int_{-h/2}^{h/2} e_{11}(z) dz \qquad (9)$$

$$L = \frac{12(1-\nu)}{Eh^3} M + \frac{12}{h^3} \int_{-h/2}^{h/2} e_{11}(z) z \, dz \qquad (10)$$

and

$$\sigma(z) = \frac{E}{1-\nu} [K + Lz - e_{11}(z)] \qquad (11)$$

The compaction or swelling of the layer in the direction perpendicular to the surface can be obtained from the strain component

$$\varepsilon_{33}(z) = e_{33}(z) - \frac{2\nu}{E} \sigma(z) \qquad (12)$$

For example, if one measures the step height between the bombarded region adjacent to a masked (and therefore undamaged) region, this is equal to the surface displacement or

$$u_3(h/2) = \int_{-h/2}^{h/2} \left[e_{33}(z') - \frac{2\nu}{E} \sigma(z') \right] dz' \qquad (13)$$

The detailed lateral stress distribution as a function of depth, as given by eqn. (11), is not easily accessible to experimental verification. However, the average or integrated stress over the depth of the damaged layer can in fact be measured by determining the curling of a bombarded specimen. To demonstrate this we compute the following average:

$$\langle \sigma \rangle = \frac{1}{\delta} \int_{h/2-\delta}^{h/2} \sigma(z) \, dz \qquad (14)$$

When performing this integration over the inelastic strain component $e_{11}(z)$, one can in fact extend it over the entire plate thickness, because $e_{11}(z) = 0$ outside the damaged layer. Therefore, the integral in eqn. (10) becomes

$$\int_{-h/2}^{h/2} z' \, e_{11}(z')dz' = \int_{h/2-\delta}^{h/2} z' \, e_{11}(z')dz' \cong \frac{1}{2}(h-\delta) \int_{h/2-\delta}^{h/2} e_{11}(z')dz'$$
$$= \frac{1}{2}(h-\delta) \int_{-h/2}^{h/2} e_{11}(z')dz' \qquad (15)$$

and using eqns. (9) and (10), one finds

$$\int_{-h/2}^{h/2} e_{11}(z')dz' = \frac{2}{(h-\delta)} \left[\frac{h^3 L}{12} - \frac{(1-\nu)M}{E} \right] \qquad (16)$$

The integral in eqn. (14) can now be evaluated, and one obtains

$$\langle \sigma \rangle = \frac{N}{h} + \frac{2M}{h\delta} - \frac{Eh^2 L}{6(1-\nu)\delta} \left[1 - 3\frac{\delta}{h}\left(1 - \frac{\delta}{h}\right) \right] \qquad (17)$$

Thus, the average lateral stress in the damaged layer of an unconstrained specimen (i.e., N=0 and M=0) is seen to be related to the plate curvature L=1/r, where r is the radius of curvature, and this parameter can easily be measured.

To evaluate eqn. (13) for the step height, we take the derivative with respect to the dose R and use the constituitive relationship (4) to obtain

$$\frac{1}{\delta}\frac{du_3}{dR} = \frac{1+\nu}{3(1-\nu)} \left\langle \frac{dS}{dR} \right\rangle - \frac{2(1-2\nu)}{3(1-\nu)} \langle \Psi\sigma \rangle \qquad (18)$$

Whereas the step height change, the term on the left hand side, can be measured directly, the rate of density change, <dS/dR>, can not. Eliminating this quantity from eqn. (18) requires two steps. We first take the derivative of eqn. (11), insert the constituitive relationship (4) and take the average over the layer thickness. The result is

$$\frac{d\langle\sigma\rangle}{dR} + \frac{E(1-\gamma)}{3(1-\nu)}\left[\left\langle\frac{dS}{dR}\right\rangle + \langle\Psi\sigma\rangle\right] = \frac{dN}{dR} + \frac{12}{h^3}\frac{dM}{dR} \qquad (19)$$

where

$$\gamma = \frac{\delta}{h} + 3\frac{\delta}{h}\left(1 - \frac{\delta}{h}\right)^2 \qquad (20)$$

Now solving eqn. (19) for <dS/dR> and substituting the result into eqn. (18) one obtains

$$\frac{1}{\delta}\frac{du_3}{dR} + \frac{1+\nu}{E(1-\gamma)}\frac{d\langle\sigma\rangle}{dR} + \langle\Psi\sigma\rangle = \frac{1-\nu}{E(1-\gamma)}\frac{d}{dR}\left[N + \frac{12}{h^3}M\right] \qquad (21)$$

For a specimen constrained from expansion and bending, or for a very thick specimen such that $h >> \delta$, the right hand side of eqn. (21) vanishes and γ becomes zero. Eqn. (21) can therefore be used to estimate radiation-induced creep from measured step heights, $u_3(R)/\delta$, and average lateral stresses, $<\sigma>$. However, the average of the quantity $\Psi\sigma$ must be factored into a product of two averages for Ψ and σ. To accomplish this it is necessary to assume a depth dependence for $\Psi(z)$ and $\sigma(z)$.

III. ANALYSIS OF EXPERIMENTAL RESULTS IN HYDROGEN-FREE VITREOUS SILICA

a) Energy Deposition Profile

The rate of density change and the radiation-induced creep rate are both proportional to the rate of energy deposition by the incident particles. For the case of 18 keV electrons which were used in the experiments of Dellin et al. [3], the energy deposition profile in glass has been computed with the SANDYL code [5], and the results are as shown in Fig. 2. This profile can be approximated by a constant value up to a depth ζ followed by an exponential decrease, as shown in the figure. Assuming the stress is also proportional to the energy deposition profile f(z), we have

$$\sigma(z, R) = \sigma_o(R) f(z) \tag{22}$$

and

$$\Psi(z, R, \sigma_{eq}) = \psi_n^o(R)\sigma_{eq}^{n-1}(z) f(z) = \psi_n^o(R)\sigma_o(R) f^n(z) \tag{23}$$

where σ_o and ψ_n^o are values in the region of nearly constant dose rate and

$$f(z) = \begin{cases} 1 & \text{for } h/2 - \zeta \le z \le h/2 \\ \exp[-(h/2 - \zeta - z)/\eta] & \text{for } h/2 - \delta \le z \le h/2 - \zeta \end{cases} \tag{24}$$

is a simple approximation to the energy deposition profile shape. The equivalent stress, σ_{eq}, is in the present case equal to the lateral stress, and this leads to the result given in eqn. (23).

According to the results shown in Fig. 2, the maximum range of the 18 keV electrons is about $\delta = 3.6$ μm, the extent of the nearly constant damage region is $\zeta = 1.76$ μm, and the exponential decay parameter is $\eta = 0.43$ μm. With the above depth distributions for the stress and the creep compliance one obtains for the average of $\Psi\sigma$ the result

$$\langle \Psi\sigma \rangle = \psi_n^o(R) \langle \sigma \rangle^n F_n = \langle \psi_n^o \rangle \langle \sigma \rangle^n \tag{25}$$

where

$$F_n = \frac{\zeta/\delta + (\eta/\delta)[1 - \exp\{-(n+1)(\delta-\zeta)/\eta\}]/(n+1)}{[\zeta/\delta + (\eta/\delta)[1 - \exp\{-(\delta-\zeta)/\eta\}]]^n} \quad (26)$$

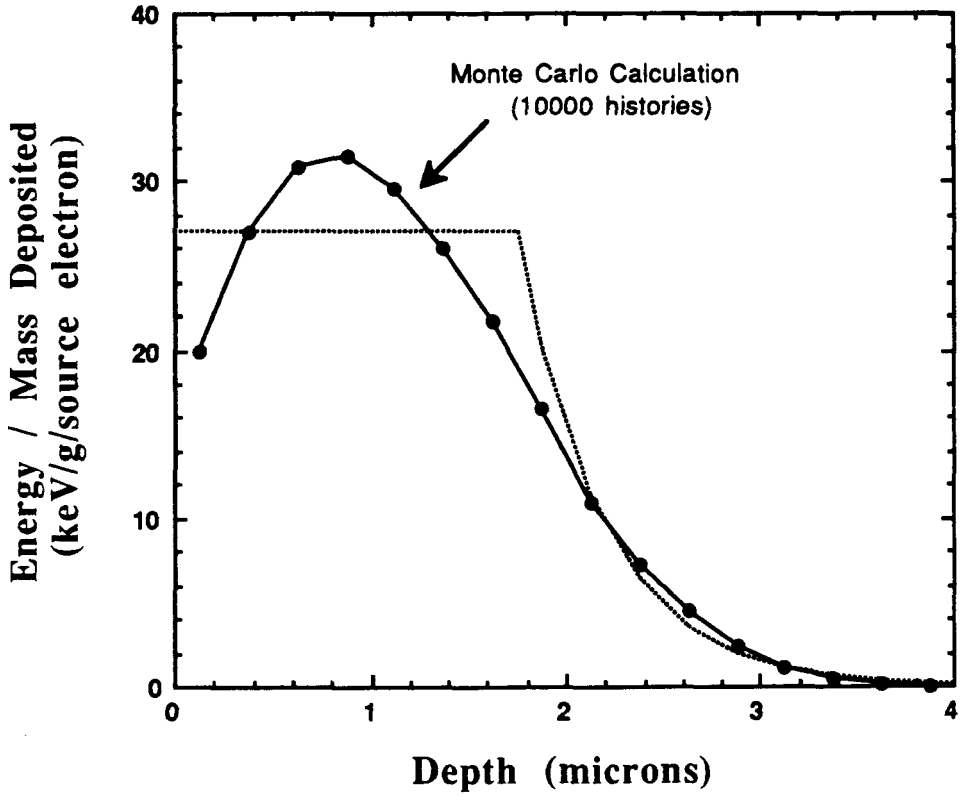

Fig. 2. Energy deposition depth profiles for 18 keV electrons impinging at normal incidence on a glass substrate. The solid line represents the exact profile and the dotted line an approximation used in the present analysis.

and where we have introduced an average creep constant $\langle\psi_n^o\rangle$. This average value differs from the actual radiation-induced creep rate constant of the material, ψ_n^o, by the constant factor F_n. Table 1 lists this factor for different values of the stress exponent, n, and it is seen that they are all of order one for low stress exponents. As a result, the average creep constant $\langle\psi_n^o\rangle$ represents a reasonably good estimate of the true creep constant ψ_n^o for $n \leq 3$.

Table 1. Ratio of average to true creep rate constants.

Stress exponent n	$\langle\psi_n^o\rangle / \psi_n^o = F_n$
1	0.9029
2	1.5950
3	2.8687
4	5.1980

b) Measurement of Step-Height

The experimental results of the investigation by Dellin, Tichenor, and Barsis [3] are shown in Figs. 3 and 4. In Fig. 3, the average and the upper and lower bounds to the measured step heights are fitted to a second order polynomial in dose, whereas a commonly used power-law fit is shown in Fig. 4 (see appendix). The former fit provides a better overall fit for the entire dose range, whereas the power-law fit is closer to the experimental data for doses below $2.0 \cdot 10^{12}$ rad. Either functional form allows direct evaluation of the derivative with respect to dose for the first term in eqn. (21).

The step height measurements of Dellin et al. were performed on samples with a thickness of h = 0.16 cm. Because $h \gg \delta$, eqn. (21) can be simplified to

$$\frac{d}{dR}\left(\frac{u_3}{\delta}\right) + \frac{1+\nu}{E}\frac{d\langle\sigma\rangle_{sh}}{dR} + \langle\psi_n^o\rangle\langle\sigma\rangle_{sh}^n = 0 \qquad (27)$$

where the subscript "sh" on the average stress indicates that it applies to the step height samples which are different from the much thinner samples employed for the stress measurements.

c) Measurement of Average Lateral Stress

In order to measure the curvature produced by the average lateral stress, Dellin et al. uniformly irradiated a thin hydrogen-free vitreous silica plate of thickness

h = 0.015 cm by a beam of 18 keV electrons. For the unconstrained specimen with no membrane load N or

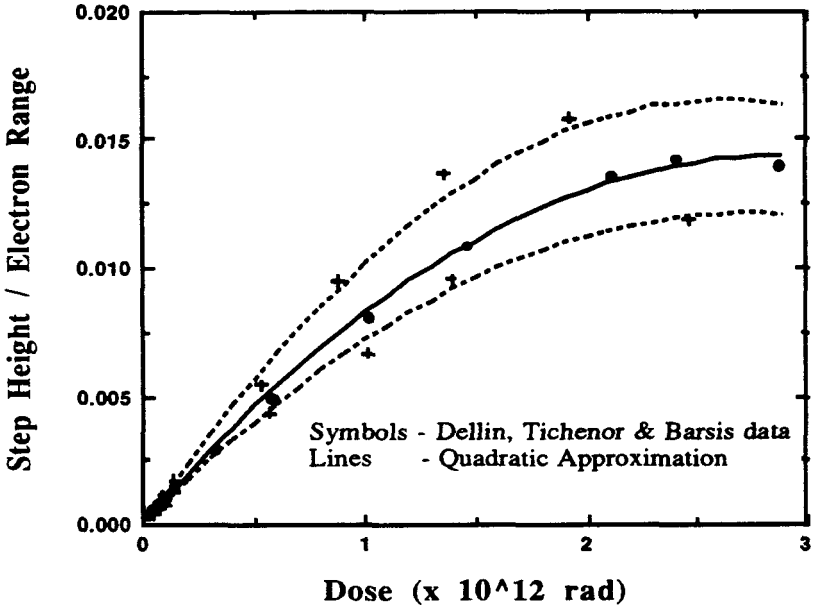

Fig. 3. Step height data (solid symbols are average values and upper and lower bounds are indicated by crosses) together with second order polynomial fits.

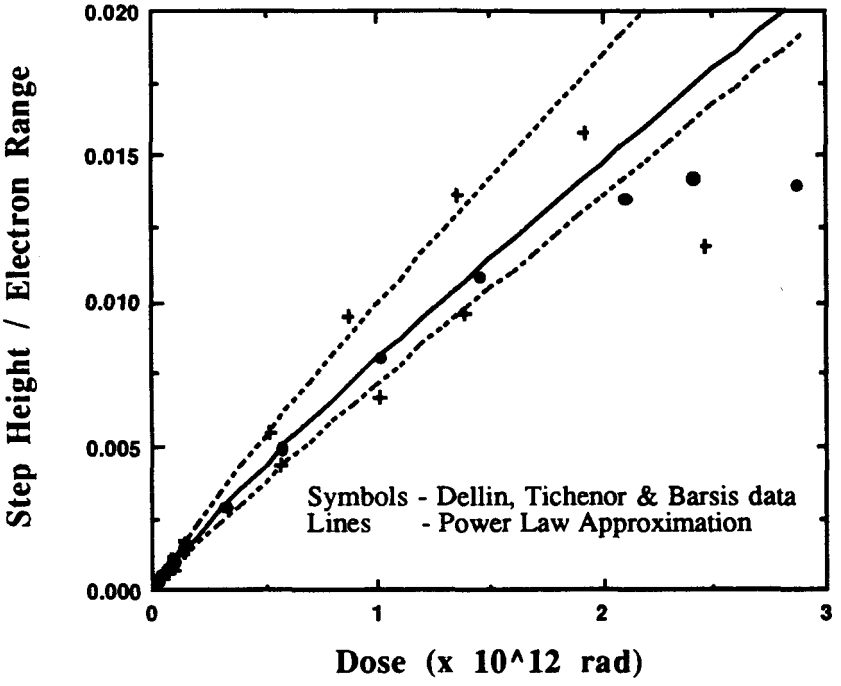

Fig. 4. Same data as in Fig.3, but fitted to a power law for doses less than $2 * 10^{12}$ rad.

bending moment M applied, eqn. (17) gives

$$\langle\sigma\rangle_b = -\frac{Eh^2}{6r\delta}\,\frac{\left[1-3\frac{\delta}{h}\left(1-\frac{\delta}{h}\right)\right]}{(1-\nu)} \qquad (28)$$

where the subscript "b" denotes the sample used for the bending measurements. Dellin et al. [3] used a relationship for the stress derived by Stoney [6] which differs from (28) by the second factor. Stoney's formula is, in fact, only valid for a thin strip rather than a plate and for the case when δ/h approaches zero. Using Poisson's ratio, $\nu = 0.17$ for vitreous silica, and electron range, $\delta = 3.2$ μm reported by Dellin et al., the second factor in eqn. (28) is equal to 1.129. We have incorporated this factor into the stress measurements given in Ref. [3], and these results are shown in Fig. 5 together with an analytical fit (see appendix) to the modified data. The derivative of the latter expression for the stress with respect to dose gives the second term in eqn. (21).

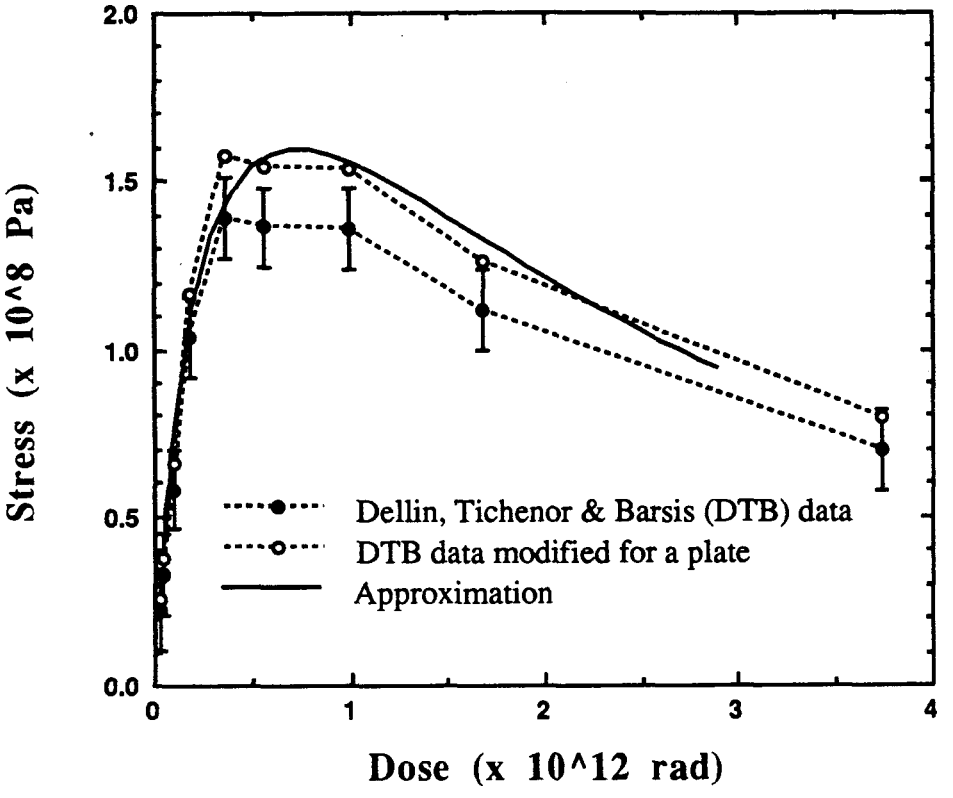

Fig. 5. Experimental results for the stress build-up in hydrogen-free vitreous silica irradiated with 18 kev electrons.

d) Determination of Radiation-Induced Creep

If the assumption is made that the average lateral stresses in the two different samples used for measuring step heights and for bending are the same for the same dose, i.e., if

$$\langle\sigma\rangle_{sh} = \langle\sigma\rangle_{b} = \langle\sigma\rangle \tag{29}$$

we can determine the average creep constant $\langle\psi_n^o\rangle$ from eqn. (27) according to

$$\langle\psi_n^o\rangle = -\frac{1}{\langle\sigma\rangle_b^n}\,\frac{d}{dR}\left[\frac{u_3}{\delta} + \frac{1+\nu}{E}\langle\sigma\rangle_b\right] \tag{30}$$

However, since the stress exponent n is unknown, eqn. (30) must be evaluated for different values of n until a nearly dose-independent creep constant is obtained. Since the stress build-up follows the densification at low doses and the two terms within the bracket of eqn. (30) nearly cancel, the values of $\langle\psi_n^o\rangle$ at doses below $0.5 \cdot 10^{12}$ rad are unreliable. The same is true for values obtained at doses above $2.0 \cdot 10^{12}$ rad, since the extrapolation for the density change is uncertain. Using this approach, the following results are obtained:

1) Assuming a linear stress dependence of radiation-induced creep, an average creep compliance $\langle\psi_1^o\rangle$ is obtained which does not seem to exhibit any dose region where it is nearly constant. Fig. 6 shows this creep compliance using the second order polynomial approximation to the step height data shown in Fig. 3; Fig. 7 uses the power-law fit of Fig. 4.

2) For a quadratic stress dependence (n=2) and the step height correlation of Fig. 3, the resulting creep constant $\langle\psi_2^o\rangle$ shown in Fig. 8 displays a nearly constant value over the dose range where eqn. (30) can be expected to be valid. Using the correlation of Fig. 4, however, does not give a satisfactory result.

3) When assuming a third power stress dependence (n=3), a nearly constant creep parameter $\langle\psi_3^o\rangle$ can again be obtained over the relevant dose range and using the step height correlation of Fig. 3. The results for this case are shown in Fig. 9. As before, unsatisfactory results are obtained with the correlation of Fig. 4.

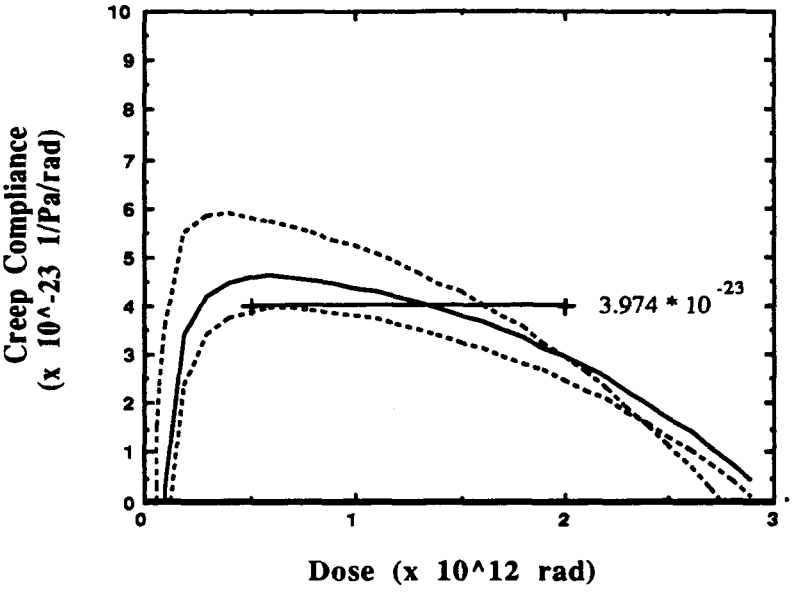

Fig. 6. Radiation-induced creep constant assuming linear stress dependence and the step height correlation displayed in Fig. 3. The horizontal line represents a mean value averaged over the indicated dose range.

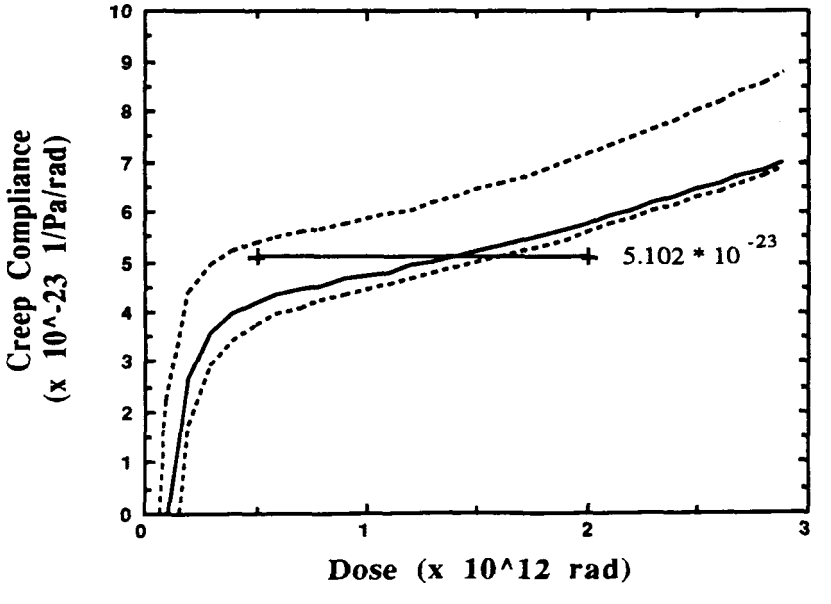

Fig. 7. Radiation-induced creep constant assuming linear stress dependence and the step height correlation displayed in Fig. 4. The horizontal line represents a mean value averaged over the indicated dose range.

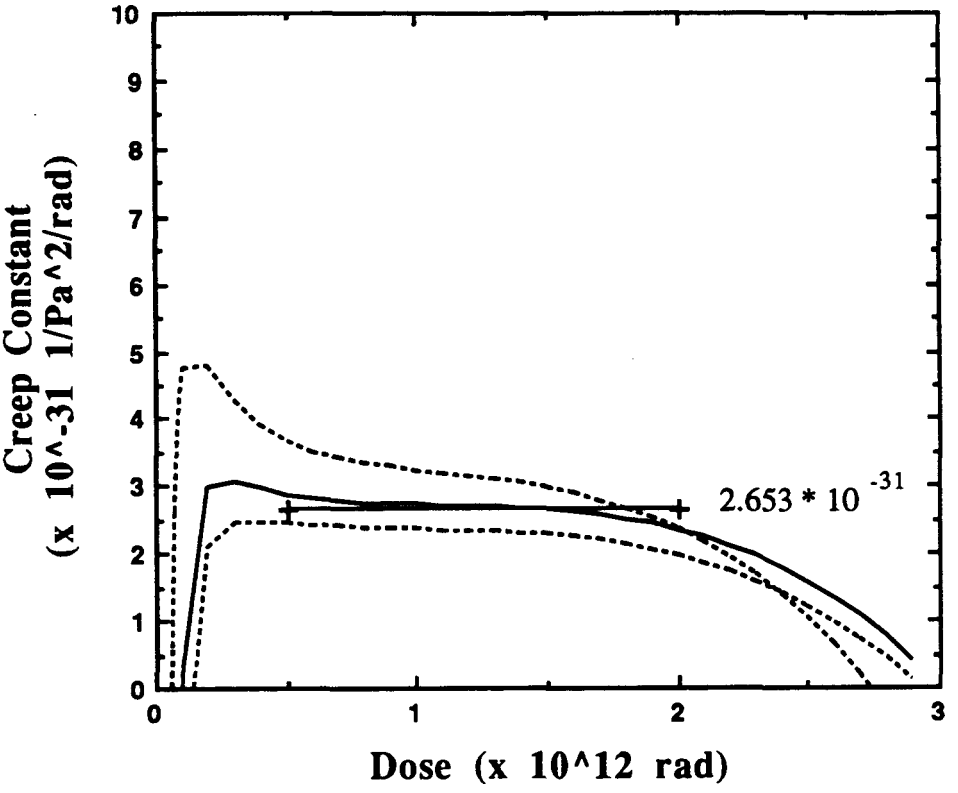

Fig. 8. Radiation-induced creep constant assuming quadratic stress dependence and the step height correlation displayed in Fig. 3. The horizontal line represents a mean value averaged over the indicated dose range.

In summary, nearly dose-independent irradiation creep parameters can be obtained when step height changes are assumed to vary with dose according to a second order polynomial, and when the radiation-induced creep rate obeys a power law relationship with a stress exponent n between two or three. The value of the radiation-induced creep constant averaged over the damaged layer is

$$\langle \psi_2^o \rangle = 2.65 \cdot 10^{-31}\ \mathrm{Pa^{-2}\ rad^{-1}} \quad \text{for } n = 2, \qquad (31)$$

or

$$\langle \psi_3^o \rangle = 1.79 \cdot 10^{-39}\ \mathrm{Pa^{-3}\ rad^{-1}} \quad \text{for } n = 3. \qquad (32)$$

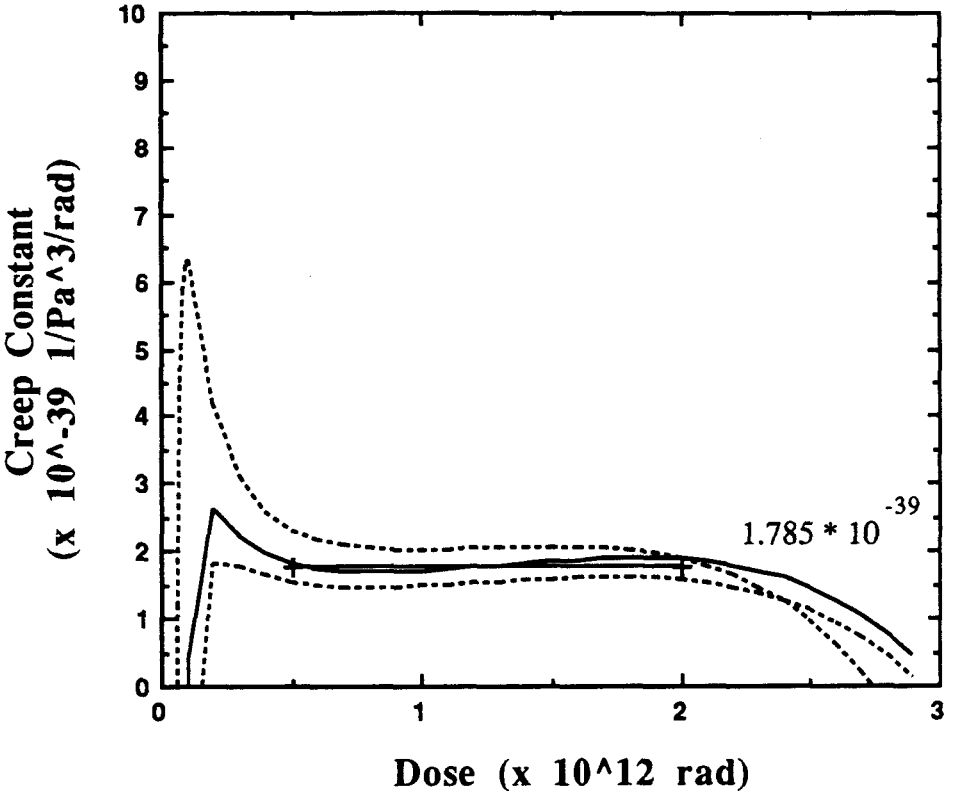

Fig. 9. Radiation-induced creep constant assuming a third power stress dependence and the step height correlation displayed in Fig. 3. The horizontal line represents a mean value averaged over the indicated dose range.

In order to test how well these dose-independent creep parameters can reproduce the lateral stress evolution, we integrate eqn. (27) with respect to the dose R using eqn. (31) or (32). As seen from Fig. 10, the calculated stresses agree very well with the experimental results except for the one data point at the highest dose.

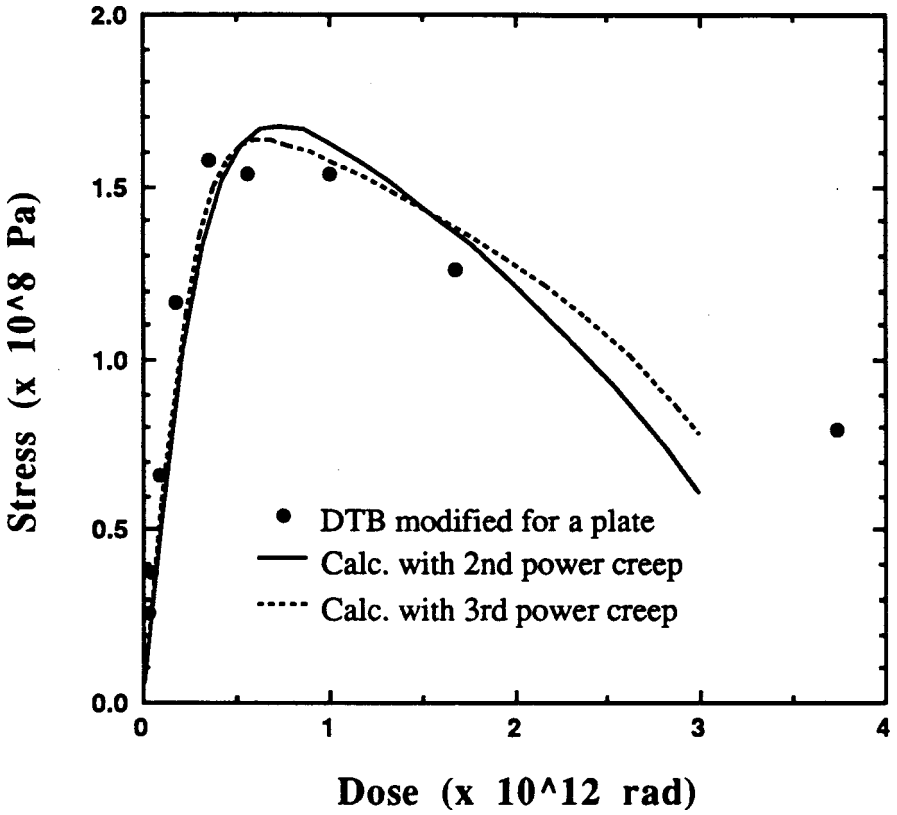

Fig. 10. Comparison of calculated stress evolution with the experimental data.

e) Relation Between Changes in Density and Step Height

As pointed out earlier, the partially constrained density changes in a thin surface layer as reflected in step height changes are different from the unconstrained density changes <S> which can only be measured directly if the entire specimen is subject to a uniform irradiation. However, the step height and unconstrained density changes are related by eqn. (18). If we use the factorization in eqn. (25), the calculated stresses shown in Fig. 10, then the integration of eqn. (18) yields the unconstrained density change presented in Fig. 11. It is seen that <S> is significantly greater then the step height (u_3/δ)
data shown as the solid symbols since, from (18),

$$\langle S \rangle \approx \frac{3(1-\nu)}{(1+\nu)} \frac{u_3}{\delta} \qquad \text{at low dose}$$

However, this difference diminishes at sufficiently high doses where step heights become equal to the unconstrained density changes, i.e.,

$$\langle S \rangle \approx \frac{u_3}{\delta} \qquad \text{at high dose}$$

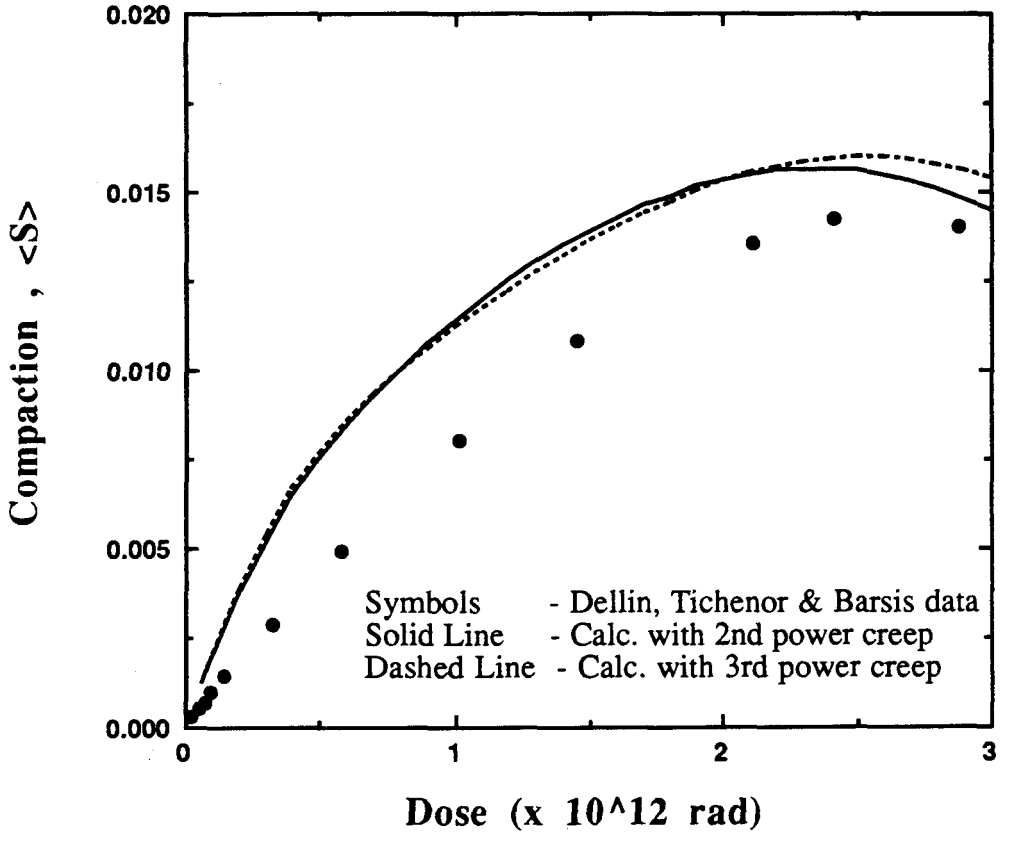

Fig. 11. Comparison of computed unconstrained density changes and measured step heights.

f) Residual Stress Relaxation

Joints between different glasses or glass and other materials often contain residual stresses as a result of differential thermal expansion. Assume such a residual stress state is biaxial and that the two principal stress components are equal. Then, eqn. (11) with K=L=0 describes the evolution of this stress with dose. If we further assume, for the purpose of illustration, that radiation produces no differential swelling in this joint, then eqn. (11) leads

to

$$\frac{d\sigma}{dR} + \frac{E\psi_n^\circ}{3(1-\nu)}\sigma^n = 0 \tag{33}$$

The solution to this equation is given by

$$\sigma(R) = \frac{\sigma_0}{\left[1 + \frac{(n-1)E\psi_n^\circ \sigma_0^{n-1} R}{3(1-\nu)}\right]^{\frac{1}{n-1}}} \tag{34}$$

where R is the dose in rads.

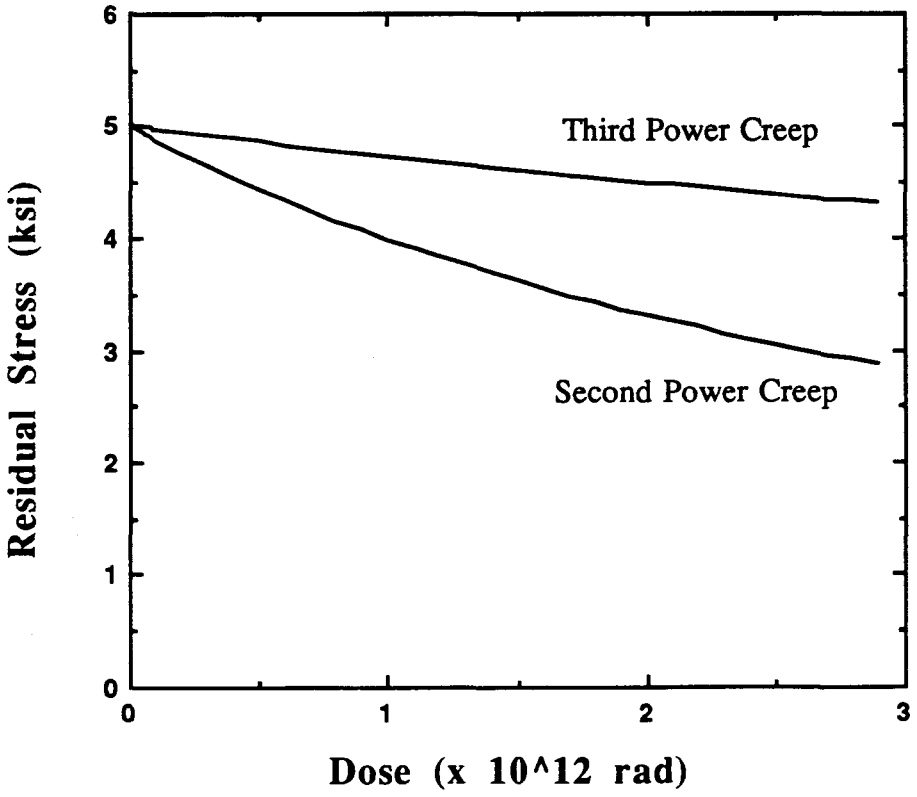

Fig. 12. Relaxation of a Residual Stress with Initial Value of 10 ksi.

If one uses eqn. (34) and the creep constants in eqns. (31) and (32) to estimate the relaxation of residual stresses with an initial value of σ_0 = 5 ksi, it is seen from Fig. 12 that they relax only by a few per cent over doses of practical interest

for the higher stress exponent of n=3, but for a stress exponent of n=2 significant stress relaxation is predicted.

III. CONCLUSIONS

The experimental observations on compaction and associated stresses produced in vitreous silica during electron irradiation can be rationalized in terms of a radiation-induced creep process. Such a process leads naturally to a saturation of the stresses produced by differential compaction or swelling long before the density saturates. Based on the known existence of radiation-induced creep in both metallic and ceramic crystalline solids, it is very probable that this effect also occurs in amorphous solids and glasses.

A comprehensive viscoelastic stress analysis has been presented for a surface layer in a plate-like specimen, when this surface layer is subject to radiation-induced density changes and radiation-induced creep. The analysis is then applied to give a new interpretation of the experimental results obtained earlier by Dellin, Tichenor, and Barsis [3].

It is found that the radiation-induced creep in vitreous silica is dependent on the stress in a non-linear fashion which can be approximated by a power law with an exponent between 2 and 3. With the obtained radiation-induced creep parameters, the difference between constrained and unconstrained density changes is quantified for the first time.

ACKNOWLEDGMENT

The authors would like to thank G.J. Thomas and D.A. Tichenor for valuable discussions.

APPENDIX

The fitting functions used to represent the measured data of Dellin et al. [3] are described in this appendix. The step height compaction data are fit both to a quadratic polynomial and, analogous to other work, a power law function. Corresponding to Fig. 3, we have for doses ranging from $2.5 * 10^{10}$ to $2.5 * 10^{12}$ rad

$$\frac{u_3}{\delta} = a_0 + a_1 R + a_2 R^2 \qquad \text{(A1)}$$

where the coefficients a_i, i = 0, 1, 2 are listed in the table below. Similarly, for the power law fits used in Fig. 4, we have

$$\frac{u_3}{\delta} = \alpha R^{\beta} \qquad \text{(A2)}$$

and the values of α and β given in Table 2 are determined for the range $2.5 * 10^{10} < R < 2.0 * 10^{12}$.

The modified stress data (see Fig. 5) is approximated by the function

$$\ln \sigma = \sum_{i=1}^{4} c_i \omega^{i-1} \qquad \text{(A3)}$$

over the dose range $2 * 10^{10} < R < 4 * 10^{12}$ where $\omega = \ln R$ and $c_1 = 323.72$, $c_2 = -40.148$, $c_3 = 1.7142$, and $c_4 = -0.0239$. To perform the numerical integration of the unconstrained density change shown in Fig. 11, linear extrapolations from the above fits are made to zero dose. In particular, we use $u_3/\delta = 3.736 * 10^{-17} R$ for $0 \le R \le 9 * 10^8$ and $\sigma = 1.1393 * 10^{-3} R$ for $0 \le R \le 2 * 10^{10}$.

Table. 2 Coefficients used in quadratic and power law fits to the step height data.

	Quadratic Fits		
	a_0	a_1	a_2
Upper Bound	-7.8930e-05	1.2602e-14	-2.3892e-27
u_3 / δ	-8.9377e-06	9.9697e-15	-1.7360e-27
Lower Bound	-8.7569e-06	8.7300e-15	-1.5729e-27
	Power Law Fits		
	α	β	
Upper Bound	1.4823e-13	0.90181	
u_3 / δ	1.5583e-13	0.89217	
Lower Bound	4.3894e-14	0.93401	

REFERENCES

[1] W.G. Wolfer, J. Nucl. Matls. **90** (1980) 713

[2] W.Primak, J. Appl. Phys. **35** (1964) 1342

[3] T.A.Dellin, D.A.Tichenor, and E.H.Barsis, J. Appl. Phys. **48** (1977) 1131

[4] T.H. Lin, *Theory of Inelastic Structures*, John Wiley & Sons, New York, 1968, Chapters 10 and 11.

[5] H.M. Colbert, *SANDYL: A Computer Program for Calculating Combined Photon-Electron Transport in Complex Systems*, SCL-DR-720109, March 1973.

[6] G.G. Stoney, Proc. Roy. Soc. (London), **A 82** (1909), 172 . A. Brenner and S. Senderoff, J. Research **42** (1949) 105, improved on Stoney's formula for situations where the layer thickness δ is a significant fraction of the strip thickness h. However, their formulae are valid only for a strip-like specimen.

UNLIMITED RELEASE
INITIAL DISTRIBUTION

New York State College of Ceramics
Attn: J.E. Shelby
Alfred University
Alfred, N.Y. 14802

0520 T.L. Buxton, MD
0520 L.D. Martin, MD
0520 C.M. Wood, MD
0520 C.M. Worley, MD
1110 S.T. Picraux
1111 B. L. Doyle
1112 S.M. Myers
1114 T.A. Michalske
1523 R.S. Chambers
1800 R.J. Eagan
1834 A.K. Hays
1840 R.E. Loehman
1845 K.D. Keefer
1845 J.W. Rogers, Jr.
1846 D.H. Doughty
2320 J.H. Renken
2321 E.F. Hartman
6454 G.L. Cano
7476 F.P. Gerstle, Jr.
7476 R.D. Watkins

8000 J. C. Crawford
Attn: E. E. Ives, 8100
R. J. Detry, 8200
P. E. Brewer, 8500
8240 C.W. Robinson
8241 G.A. Benedetti
8241 V.N. Kaliakin
8241 J.C. Keilman
8300 P.L. Mattern
8312 M.I. Baskes
8340 W. Bauer
8341 A.J. Antolak (10)
8341 W.G. Wolfer (10)
8343 G.J. Thomas
8347 A.E. Pontau
8400 R.C. Wayne
8440 H. Hanser
8446 J.L. Handrock
8446 B.L. Haroldson
8446 D.A. Tichenor

8446 K. Wally
8446 A.J. West
8540 R.W. Rohde

8535 Publications for OSTI (10)

8535 Publications/Technical
Library Processes Div. (3)

3141 Technical Library
Processes Div. (3)

8524-2 Central Technical Files (3)